3DOF Wheelchair Mounted Robotic Arm Exoskeleton

Thesis Defense

Allen Tan

Advisor: Dr. Kee Moon

Department of Mechanical Engineering

San Diego State University

June 12, 2015

Overview

- Introduction
- Background/Literature Review
- Equipment
- Design
- Kinematic Modeling
- Dynamic Modeling
- PID Controller
- Gravity Compensation
- Determination of User Intent
- Conclusion
- Future Work

Introduction

- Robotic Arm
  - 3 DOF
    - 2 at Shoulder
    - 1 at Elbow
  - Mounted on wheelchair

- Goal of Research:
  - Design a **lightweight** robotic arm exoskeleton

Robotic arm attached to wheelchair with user.

Background: History of Robotics

- Definition of Robot
  - Comes from Czech word "robota," which means serf labor
- First mention of robot in Homer's *Illiad*
  - Handmaidens for Hephaestus
- First industrial robot in 1961 - Unimate
  - Used at General Motors (GE) for automobiles

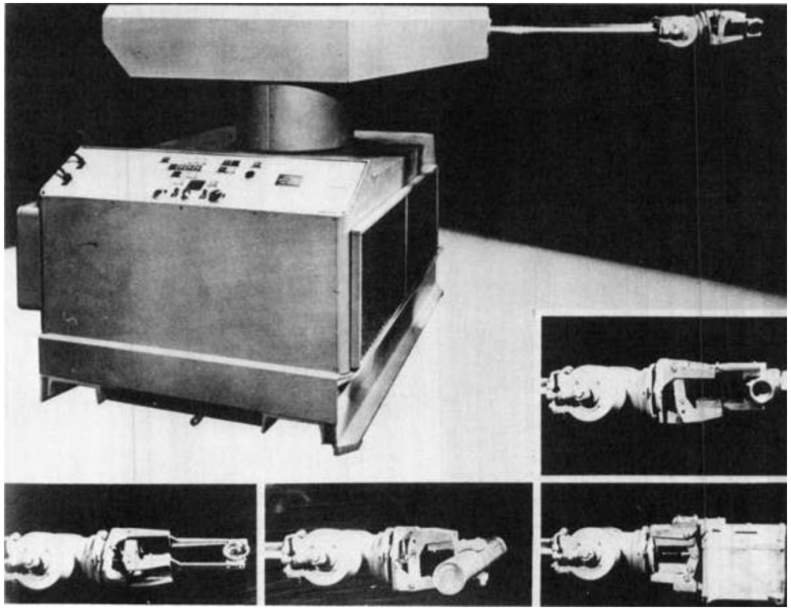

Unimate in General Motors factory[1].

1. Engelberger, Joseph F. "Historical Perspective of Industrial Robotics." In Handbook of Industrial Robots, edited by Shimon F. Nof, xvii-xviii. New York: John Wiley & Sons, 1985.

Background: Wearable Robots

- Definition
  - Improves and/or restores functionality of limb
- Three types
  - Empowering Robotic Exoskeletons
    - HAL (Hybrid Assistive Limb)
  - Orthotic Robots
    - ARMin
  - Prosthetic Robots
    - DEKA Arm

Dr. Sankai with HAL[2].

DEKA Arm used to drink water[3].

2. Sankai, Yoshiyuki. "Leading Edge of Cybernics: Robot Suit HAL." Paper presented at the 2006 SICE-ICASE International Joint Conference, Busan, South Korea, October 18-21, 2006.
3. DEKA Research and Development Corporation. "The DEKA Arm." http://www.dekaresearch.com/deka arm.shtml.

Equipment: Dynamixel MX-64R

Overview

- Features
  - Built-in PID controller
  - Daisy-chain wiring
- Properties
  - Dimensions:
    40.2mm x 61.1 mm x 41mm
  - Weight: 135 g
  - Resolution 0.088°
  - Gear Ratio: 200:1
  - Stall Torque: 6 Nm
    - Recommended: 1.2 Nm
  - Max Speed: 63 rpm

MX-64R actuator[4].

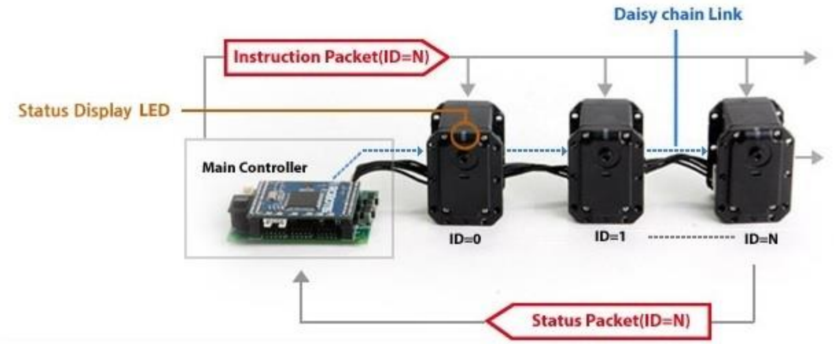

Daisy-chain of Dynamixels[5].

4. ROBO- TIS. “MX-64T / MX- 64R e-Manual.” http://support.robotis.com /en/product/dynamixel/mx series/mx-64.htm.
5. ROBOTIS. “Dynamixel.” http://www.robotis.com/xe/dynamixel en.

Equipment: Delsys Trigno

Overview

- System for Surface Electromyography (sEMG)
- Features
  - Wireless
  - Rechargeable Battery
  - Built-in Accelerometers
- Properties
  - Transmission Range: 20 m
  - EMG Signal Sampling Rate: 2000 samples/sec
  - EMG Signal Resolution: 16-bit

Delsys Trigno system[6].

6. Delsys. "Trigno Wireless System User's Guide." https://www.delsys.com/Attachments pdf/Trigno %20Wireless%20System%20Users%20Guide %20%28MAN-012-2-3%29.pdf.

Equipment: Delsys Trigno

How It Works

Sensor Placement

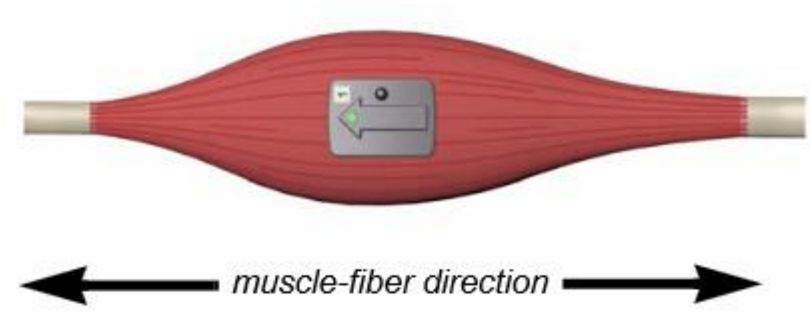

Trigno sensor placement[7].

EMG Output

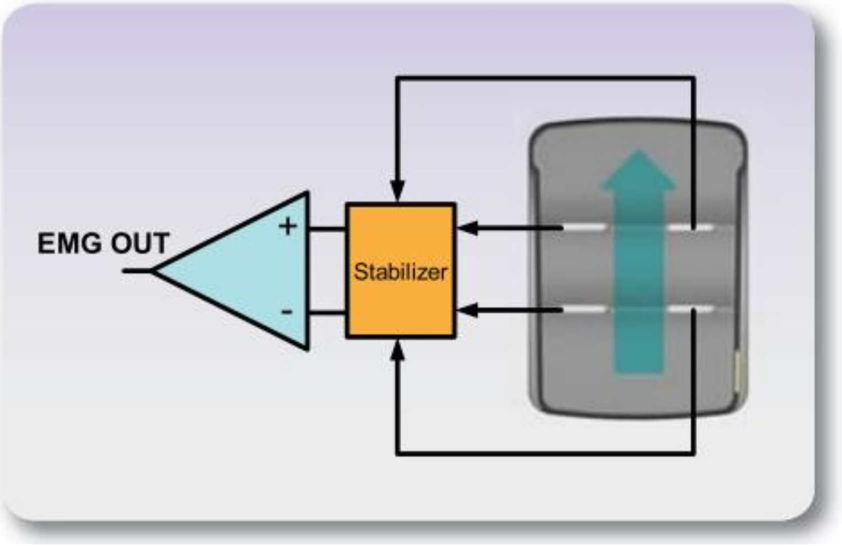

Trigno EMG detection[8].

7. Delsys. "Trigno Wireless System User's Guide." https://www.delsys.com/Attachments pdf/Trigno %20Wireless%20System%20Users%20Guide %20%28MAN-012-2-3%29.pdf.
8. Delsys. "Trigno Wire- less - FAQ." https://www.delsys.com/Attachments pdf/Trigno %20FAQ%20%28DOC-208-1-0%29-web.pdf.

Design: Frame

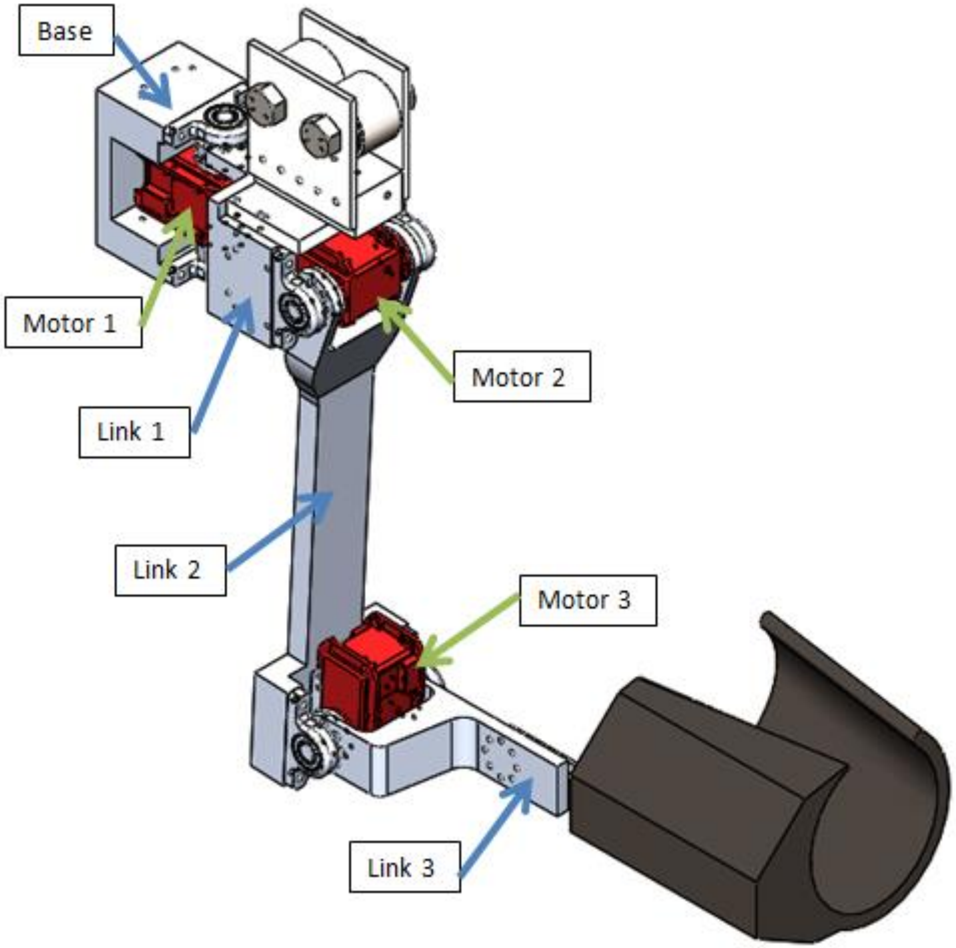

Annotated CAD model of robotic arm.

Design: Arm Movements

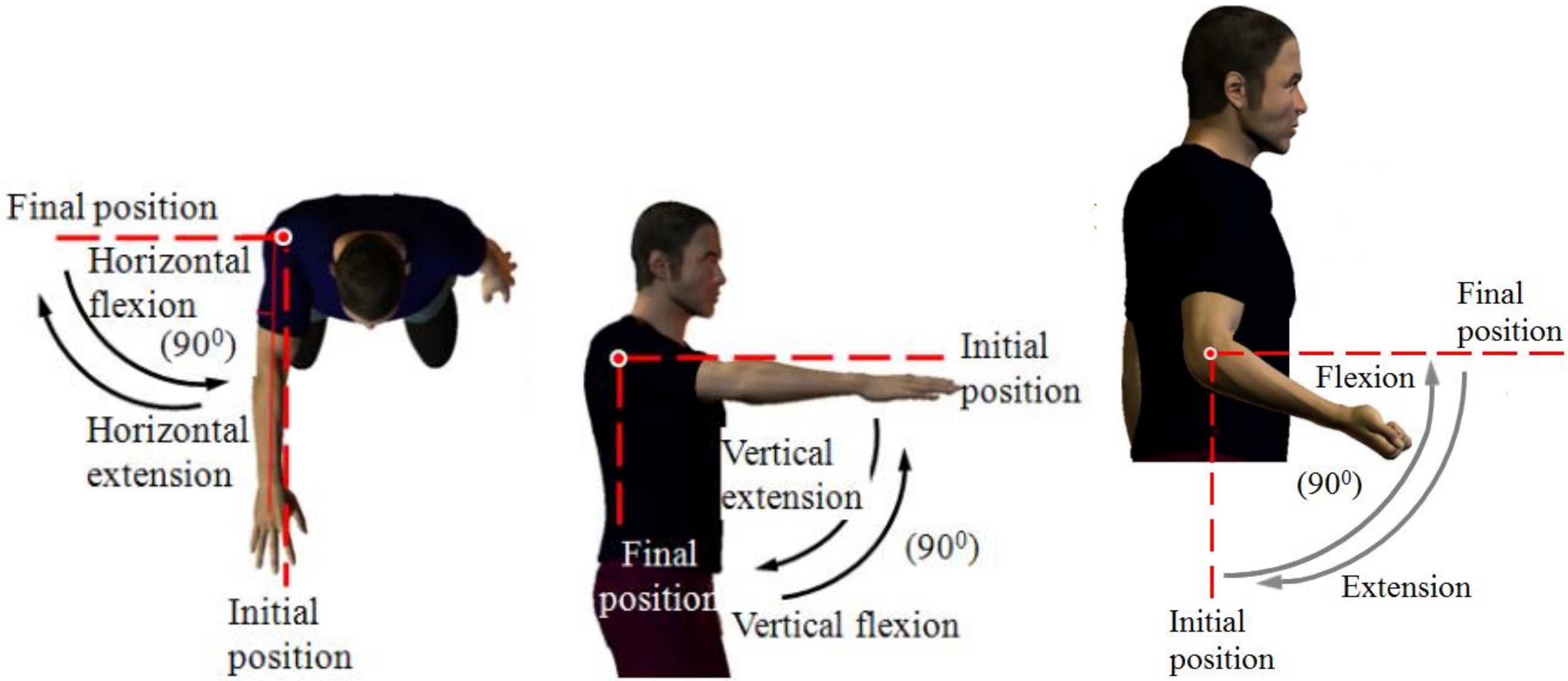

(a) Shoulder horizontal (b) Shoulder vertical (c) elbow

Desired Arm Movements Possible with 3DOF Robotic Arm[9].

9. Gopura, R.A.R.C. “A Study on Human Upper-Limb Muscles Activities.” International Journal of Bioelectro- magnetism 12, no. 2 (2010): 54-61.

Design: Safety

- Safety Features
  - Physical Stops

Joint	Minimum Joint Angle (deg)	Maximum Joint Angle (deg)
1	-90	90
2	-102.78	66.57
3	-20.91	100.61

  - Stops Through Software

Joint	Minimum Joint Angle (deg)	Maximum Joint Angle (deg)
1	-90	0
2	-90	0
3	0	-90

  - No straps

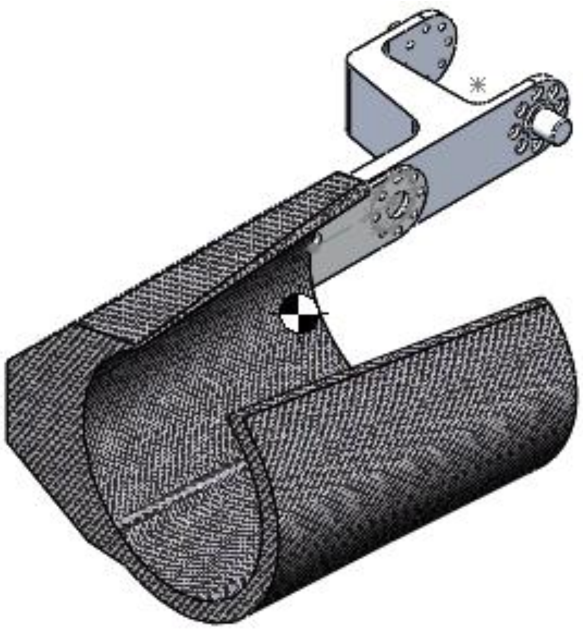

Arm cuff as part of link 3.

Kinematic Modeling: Theory

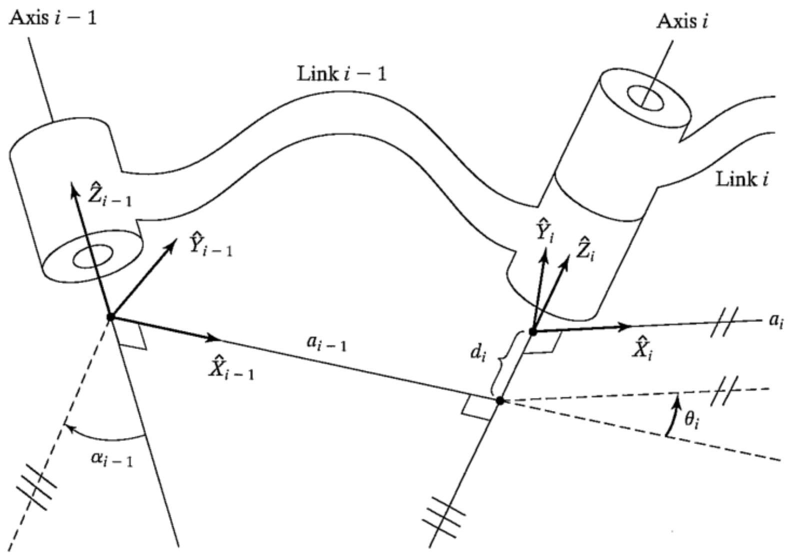

Modified Denavit-Hartenberg parameters[10].

Find position on robot w.r.t. Global Frame 0: $^{0}r_p = {}^{0}T_B \, {}^{n}r_p$ (1)

Series of Transformation Matrices: $^{0}T_B = {}^{0}T_1(q_1)\, {}^{1}T_2(q_2)\, {}^{2}T_3(q_3) \ldots {}^{n-1}T_n(q_n)$ (2)

Modified DH:

$$^{i-1}T_i = R_{x_i,\alpha_{i-1}} D_{x_i,a_{i-1}} R_{z_i,\theta_i} D_{z_i,d_i} = \begin{bmatrix} \cos\theta_i & -\sin\theta_i & 0 & a_{i-1} \\ \sin\theta_i\cos\alpha_{i-1} & \cos\theta_i\cos\alpha_{i-1} & -\sin\alpha_{i-1} & -\sin\alpha_{i-1}d_i \\ \sin\theta_i\sin\alpha_{i-1} & \cos\theta_i\sin\alpha_{i-1} & \cos\alpha_{i-1} & \cos\alpha_{i-1}d_i \\ 0 & 0 & 0 & 1 \end{bmatrix} \quad (3)$$

10. Modified Denavit-Hartenberg parameters. Source: Craig, John J. Introduction to Robotics: Mechanics and Control. 3rd ed. Upper Saddle River: Prentice Hall, 2004.

Kinematic Modeling: Parameters

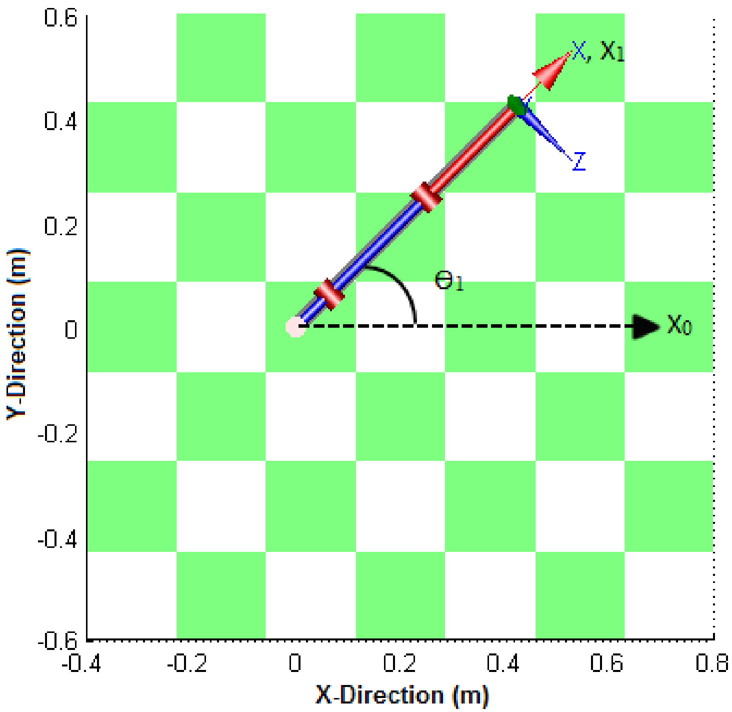

Joint 1 angle.

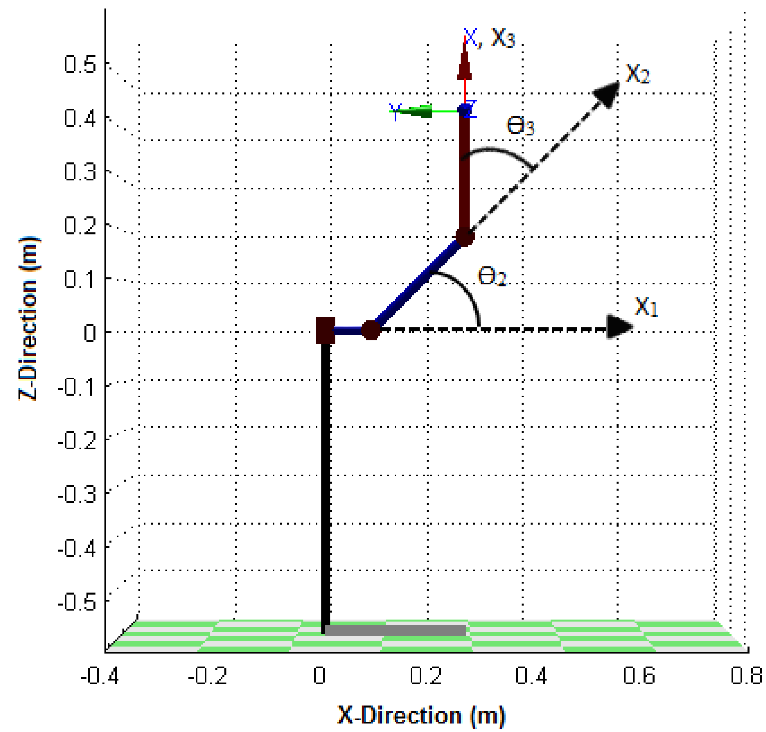

Joint 2 and joint 3 angles.

Modified DH Link Parameters.

i	a_{i-1} (cm)	α_{i-1} (deg)	d_i (cm)	θ_i (deg)
1	0	0	0	θ_1
2	8.9954	90	0	θ_2
3	26.1213	0	0	θ_3

Kinematic Modeling: Workspace

X-Y Plane

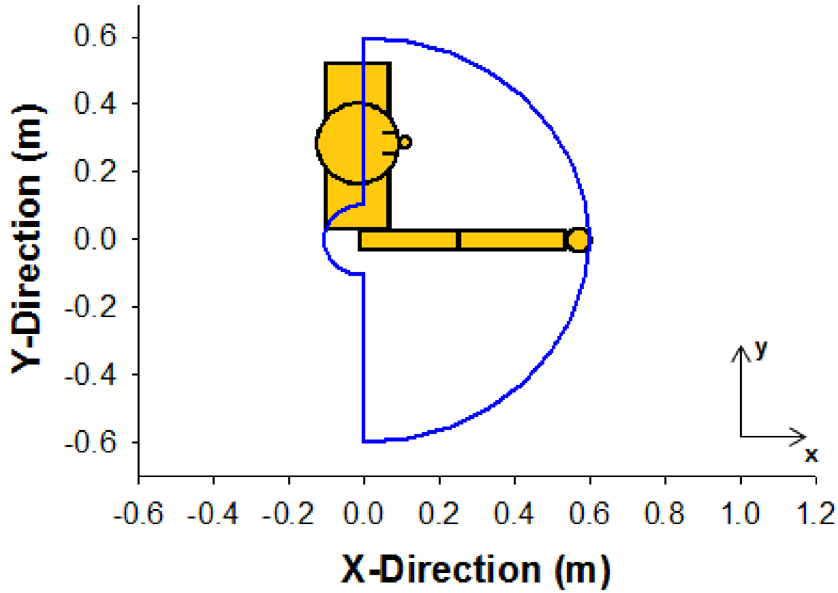

End-effector workspace in X-Y plane.

X-Z Plane

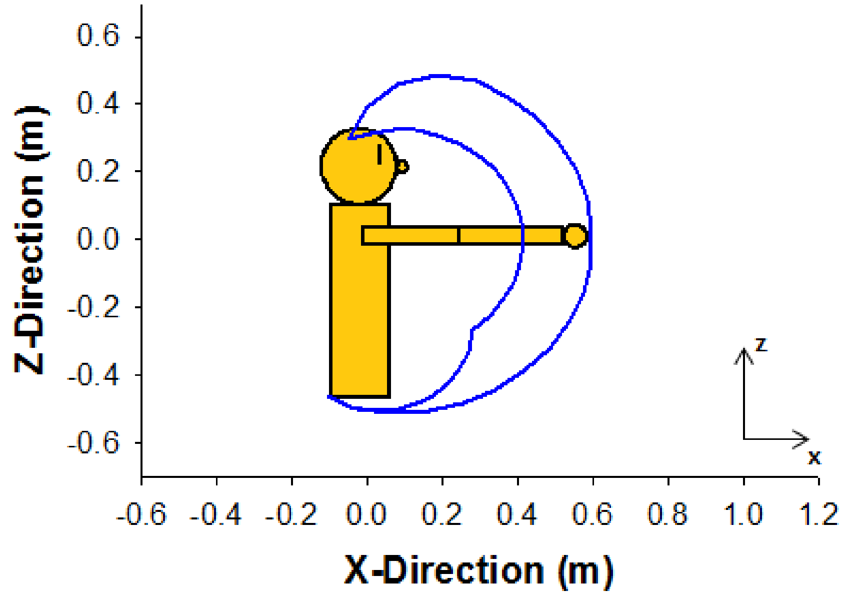

End-effector workspace in X-Z plane.

Dynamic Modeling: Theory

Lagrangian: $$L(q,\dot{q}) = T(q,\dot{q}) - U(q) \quad (4)$$

Total Kinetic Energy for Link *i*: $$T_i = \frac{1}{2}(m_i v_{C_i}^T v_{C_i} + \omega_i^T \, {}^0I_{C_i} \omega_i) \quad (5)$$

Sum of Total Kinetic Energies: $$T = \sum_{i=1}^{n} T_i \quad (6)$$

Potential Energy for Link *i*: $$U_i = m_i(-g^T p_{c_i}) \quad (7)$$

Sum of Potential Energies: $$U = \sum_{i=1}^{n} U_i \quad (8)$$

Euler-Lagrange: $$\frac{d}{dt}\left[\frac{\partial L(q,\dot{q})}{\partial \dot{q}_i}\right] - \frac{\partial L(q,\dot{q})}{\partial q_i} = \tau_i, \qquad i = 1, \cdots, n \quad (9)$$

Dynamic Modeling: Joint Torques

Motor 1

$$
\begin{aligned}
\tau_1 = \ddot{\theta}_1 \Bigg[& m_1 \frac{l_1^2}{4} + I_{zz_1} + m_2 \left(l_1 + \frac{l_2}{2} c\theta_2 \right)^2 + I_{xx_2} s^2\theta_2 + I_{yy_2} c^2\theta_2 + I_{xy_2} s(2\theta_2) \\
& + m_3 \left(l_1^2 + l_2^2 c^2\theta_2 + \frac{l_3^2}{4} c^2\theta_{23} + 2 l_1 l_2 c\theta_2 + l_1 l_3 c\theta_{23} + l_2 l_3 c\theta_2 c\theta_{23} \right) \\
& + I_{xx_3} s^2\theta_{23} + I_{yy_3} c^2\theta_{23} + I_{xy_3} s(2\theta_{23}) \Bigg] \\
+ \dot{\theta}_2 \Bigg\{ & - m_2 \dot{\theta}_1 l_2 \left(l_1 + \frac{l_2}{2} c\theta_2 \right) s\theta_2 + 2\dot{\theta}_1 I_{xx_2} c\theta_2 s\theta_2 - 2\dot{\theta}_1 I_{yy_2} c\theta_2 s\theta_2 \\
& + 2\dot{\theta}_1 I_{xy_2} c2\theta_2 + \dot{\theta}_2 I_{xz_2} c\theta_2 - \dot{\theta}_2 I_{yz_2} s\theta_2 \\
& + m_3 \dot{\theta}_1 \left[-2 l_2^2 c\theta_2 s\theta_2 - \frac{l_3^2}{4} c\theta_{23} s\theta_{23} - 2 l_1 l_2 s\theta_2 - l_1 l_3 s\theta_{23} - l_2 l_3 s(2\theta_2 + \theta_3) \right] \\
& + 2\dot{\theta}_1 I_{xx_3} c\theta_{23} s\theta_{23} - 2\dot{\theta}_1 I_{yy_3} c\theta_{23} s\theta_{23} + 2\dot{\theta}_1 I_{xy_3} c(2\theta_{23}) \\
& + (\dot{\theta}_2 + \dot{\theta}_3) I_{xz_3} c\theta_{23} - (\dot{\theta}_2 + \dot{\theta}_3) I_{yz_3} s\theta_{23} \Bigg\} \\
+ \ddot{\theta}_2 & \left[I_{xz_2} s\theta_2 + I_{yz_2} c\theta_2 + I_{xz_3} s\theta_{23} + I_{yz_3} c\theta_{23} \right] \\
+ \dot{\theta}_3 \Bigg[& - m_3 \dot{\theta}_1 \left(\frac{l_3^2}{2} c\theta_{23} s\theta_{23} + l_1 l_3 s\theta_{23} + l_2 l_3 c\theta_2 s\theta_{23} \right) + 2\dot{\theta}_1 I_{xx_3} c\theta_{23} s\theta_{23} \\
& - 2\dot{\theta}_1 I_{yy_3} c\theta_{23} s\theta_{23} + 2\dot{\theta}_1 I_{xy_3} c(2\theta_{23}) + (\dot{\theta}_2 + \dot{\theta}_3) I_{xz_3} c\theta_{23} - (\dot{\theta}_2 + \dot{\theta}_3) I_{yz_3} s\theta_{23} \Bigg] \\
+ \ddot{\theta}_3 & \left[I_{xz_3} s\theta_{23} + I_{yz_3} c\theta_{23} \right]
\end{aligned}
\tag{10}
$$

Dynamic Modeling: Joint Torques

Motor 2

$$
\begin{aligned}
\tau_2 = {} & \ddot{\theta}_1 \left[I_{xz_2} s\theta_2 + I_{yz_2} c\theta_2 + I_{xz_3} s\theta_{23} + I_{yz_3} c\theta_{23} \right] \\
& + \dot{\theta}_2 \left[\dot{\theta}_1 I_{xz_2} c\theta_2 - \dot{\theta}_1 I_{yz_2} s\theta_2 + \dot{\theta}_1 I_{xz_3} c\theta_{23} - \dot{\theta}_1 I_{yz_3} s\theta_{23} \right] \\
& + \ddot{\theta}_2 \left[m_2 \frac{l_2^2}{4} + m_3 \left(l_2^2 + l_2 l_3 c\theta_3 + \frac{l_3^2}{4} \right) + I_{zz_2} + I_{zz_3} \right] \\
& + \dot{\theta}_3 \left[-\frac{1}{2} m_3 l_2 l_3 s\theta_3 (2\dot{\theta}_2 + \dot{\theta}_3) + \dot{\theta}_1 I_{xz_3} c\theta_{23} - \dot{\theta}_1 I_{yz_3} s\theta_{23} \right] \\
& + \ddot{\theta}_3 \left[\frac{1}{2} m_3 l_3 \left(l_2 c\theta_2 + \frac{l_3}{2} \right) + I_{zz_3} \right] \\
& + m_2 \dot{\theta}_1 \frac{l_2}{2} \left(l_1 + \frac{l_2}{2} c\theta_2 \right) s\theta_2 - \dot{\theta}_1^2 I_{xx_2} c\theta_2 s\theta_2 + \dot{\theta}_1^2 I_{yy_2} c(2\theta_2) s\theta_2 \\
& - \dot{\theta}_1^2 I_{xy_2} c(2\theta_2) - \dot{\theta}_1 \dot{\theta}_2 I_{xz_2} c\theta_2 + \dot{\theta}_1 \dot{\theta}_2 I_{yz_2} s\theta_2 \\
& + \frac{1}{2} m_3 \dot{\theta}_1^2 \left[2 l_2^2 c\theta_2 s\theta_2 + \frac{l_3^2}{2} c\theta_{23} s\theta_{23} + 2 l_1 l_2 s\theta_2 + l_1 l_3 s\theta_{23} + l_2 l_3 s(2\theta_2 + \theta_3) \right] \\
& - \dot{\theta}_1^2 I_{xx_3} c\theta_{23} s\theta_{23} + \dot{\theta}_1^2 I_{yy_3} c\theta_{23} s\theta_{23} - \dot{\theta}_1^2 I_{xy_3} c(2\theta_{23}) \\
& - \dot{\theta}_1 (\dot{\theta}_2 + \dot{\theta}_3) I_{xz_3} c\theta_{23} + \dot{\theta}_1 (\dot{\theta}_2 + \dot{\theta}_3) I_{yz_3} s\theta_{23} + m_2 g \frac{l_2}{2} c\theta_2 + m_3 g \left(l_2 c\theta_2 + \frac{l_3}{2} c\theta_{23} \right)
\end{aligned}
\tag{11}
$$

Dynamic Modeling: Joint Torques

Motor 3

$$
\begin{aligned}
\tau_3 =& \ddot{\theta}_1 \left[I_{xz_3} s\theta_{23} + I_{yz_3} c\theta_{23} \right] \\
&+ \dot{\theta}_2 \left[\dot{\theta}_1 I_{xz_3} c\theta_{23} - \dot{\theta}_1 I_{yz_3} s\theta_{23} \right] + \ddot{\theta}_2 \left[m_3 \frac{l_3}{2} \left(l_2 c\theta_2 + \frac{l_3}{2} \right) + I_{zz_3} \right] \\
&+ \dot{\theta}_3 \left[-m_3 \dot{\theta}_2 l_2 \frac{l_3}{2} s\theta_3 + \dot{\theta}_1 I_{xz_3} c\theta_{23} - \dot{\theta}_1 I_{yz_3} s\theta_{23} \right] + \ddot{\theta}_3 \left[m_3 \frac{l_3^2}{4} + I_{zz_3} \right] \\
&+ \frac{1}{2} m_3 \left[\dot{\theta}_1^2 \left(\frac{l_3^2}{2} c\theta_{23} s\theta_{23} + l_1 l_3 s\theta_{23} + l_2 l_3 c\theta_2 s\theta_{23} \right) + \dot{\theta}_2^2 l_2 l_3 s\theta_3 + \dot{\theta}_2 \dot{\theta}_3 l_2 l_3 s\theta_3 \right] \\
&- \dot{\theta}_1^2 I_{xx_3} c\theta_{23} s\theta_{23} + \dot{\theta}_1^2 I_{yy_3} c\theta_{23} s\theta_{23} - \dot{\theta}_1^2 I_{xy_3} c(2\theta_{23}) \\
&- \dot{\theta}_1 (\dot{\theta}_2 + \dot{\theta}_3) I_{xz_3} c\theta_{23} + \dot{\theta}_1 (\dot{\theta}_2 + \dot{\theta}_3) I_{yz_3} s\theta_{23} + m_3 g \frac{l_3}{2} c\theta_{23}
\end{aligned}
\tag{12}
$$

Dynamic Modeling: Linearization

Joint Accelerations:

$$\ddot{\theta} = M^{-1}\left[\tau - C(\theta, \dot{\theta}) - G(\theta)\right] \quad (13)$$

Variables for Acceleration of Joint *i*:

$$\ddot{\theta}_i = f\left(\theta_1, \theta_2, \theta_3, \dot{\theta}_1, \dot{\theta}_2, \dot{\theta}_3, \tau_1, \tau_2, \tau_3\right) \quad (14)$$

Equilibrium Point:

$$x^* = \begin{Bmatrix} \theta_{1_{eq}} \\ \theta_{2_{eq}} \\ \theta_{3_{eq}} \\ \dot{\theta}_{1_{eq}} \\ \dot{\theta}_{2_{eq}} \\ \dot{\theta}_{3_{eq}} \end{Bmatrix} = \begin{Bmatrix} 0 \\ -\frac{\pi}{2} \\ 0 \\ 0 \\ 0 \\ 0 \end{Bmatrix} \quad (15)$$

Taylor Series Approximation:

$$\ddot{\theta}_{i_{lin}} = \ddot{\theta}_i(x^*) + \frac{d\ddot{\theta}_i}{dx}(x - x^*), \text{ where } x = \begin{Bmatrix} \theta_1 \\ \theta_2 \\ \theta_3 \\ \dot{\theta}_1 \\ \dot{\theta}_2 \\ \dot{\theta}_3 \end{Bmatrix} \quad (16)$$

Dynamic Modeling: State-Space

General State-Space Form:

$$\dot{\bar{x}} = [A]\bar{x} + [B]\tau \quad (17)$$

$$y = [C]\bar{x} + [D]\tau \quad (18)$$

State Vector ($\bar{x}$):

$$\bar{x} = x - x^* = \begin{Bmatrix} \theta_1 \\ \theta_2 \\ \theta_3 \\ \dot{\theta}_1 \\ \dot{\theta}_2 \\ \dot{\theta}_3 \end{Bmatrix} - \begin{Bmatrix} 0 \\ -\frac{\pi}{2} \\ 0 \\ 0 \\ 0 \\ 0 \end{Bmatrix} \quad (19)$$

State-Space Form of 3DOF System:

$$\begin{Bmatrix} \dot{\theta}_1 \\ \dot{\theta}_2 \\ \dot{\theta}_3 \\ \ddot{\theta}_1 \\ \ddot{\theta}_2 \\ \ddot{\theta}_3 \end{Bmatrix} = \begin{bmatrix} 0 & 0 & 0 & 1 & 0 & 0 \\ 0 & 0 & 0 & 0 & 1 & 0 \\ 0 & 0 & 0 & 0 & 0 & 1 \\ 0 & -0.0955 & 0.7283 & 0 & 0 & 0 \\ 0 & -52.5498 & 62.9780 & 0 & 0 & 0 \\ 0 & 83.5340 & -270.7207 & 0 & 0 & 0 \end{bmatrix} \begin{Bmatrix} \theta_1 \\ \theta_2 + \frac{\pi}{2} \\ \theta_3 \\ \dot{\theta}_1 \\ \dot{\theta}_2 \\ \dot{\theta}_3 \end{Bmatrix} + \begin{bmatrix} 0 & 0 & 0 \\ 0 & 0 & 0 \\ 0 & 0 & 0 \\ 71.3072 & 0.3689 & -1.6052 \\ 0.3689 & 51.7315 & -158.6295 \\ -1.6052 & -158.6295 & 618.1473 \end{bmatrix} \quad (20)$$

Dynamic Modeling: Linear Model
Comparison with Non-linear Model – Motor 1

Initial Joint 3 Angle of 5°

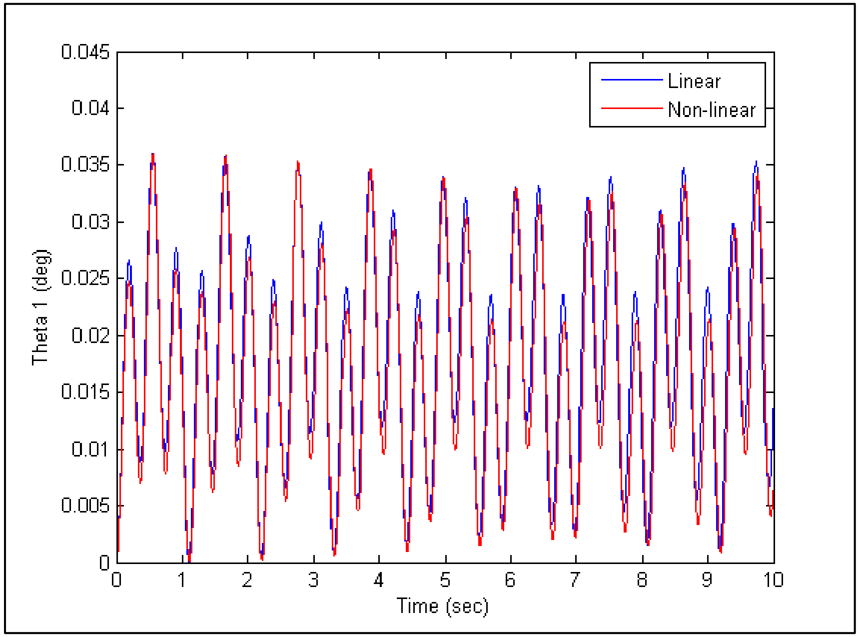

Response of joint 1 due to a non-equilibrium initial joint 3 angle of 5 degrees.

Initial Joint 3 Angle of 10°

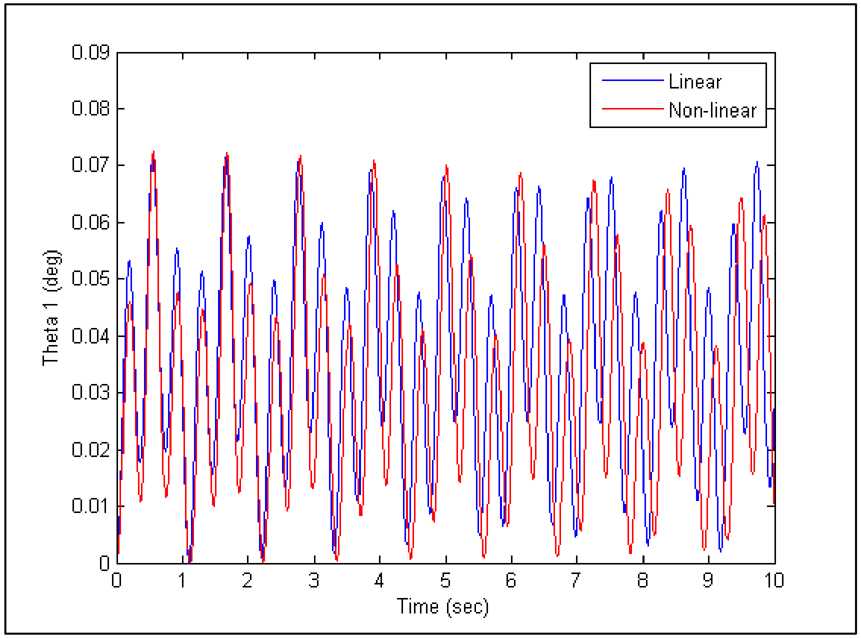

Response of joint 1 due to a non-equilibrium initial joint 3 angle of 10 degrees.

Dynamic Modeling: Linear Model

Comparison with Non-linear Model – Motor 2

Initial Joint 3 Angle of 5°

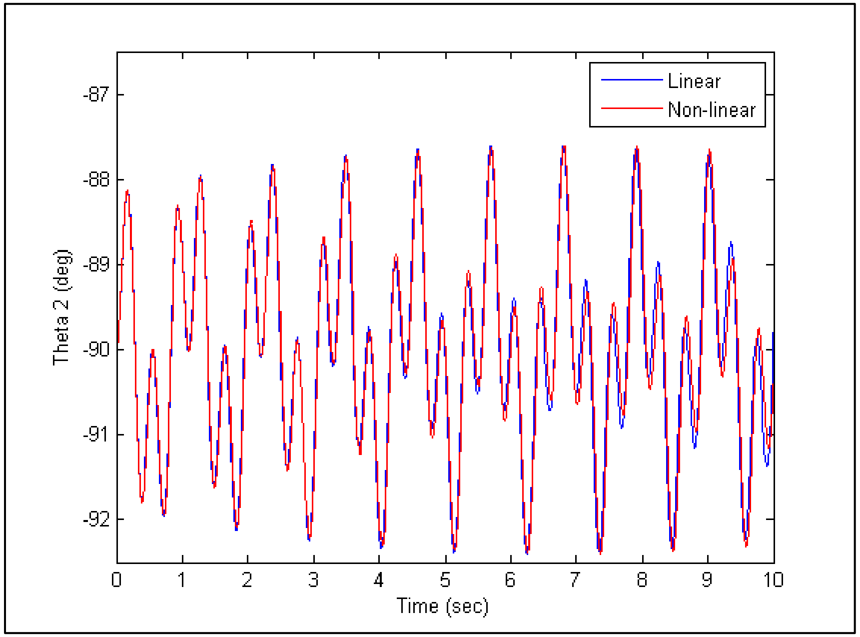

Response of joint 2 due to a non-equilibrium initial joint 3 angle of 5 degrees.

Initial Joint 3 Angle of 10°

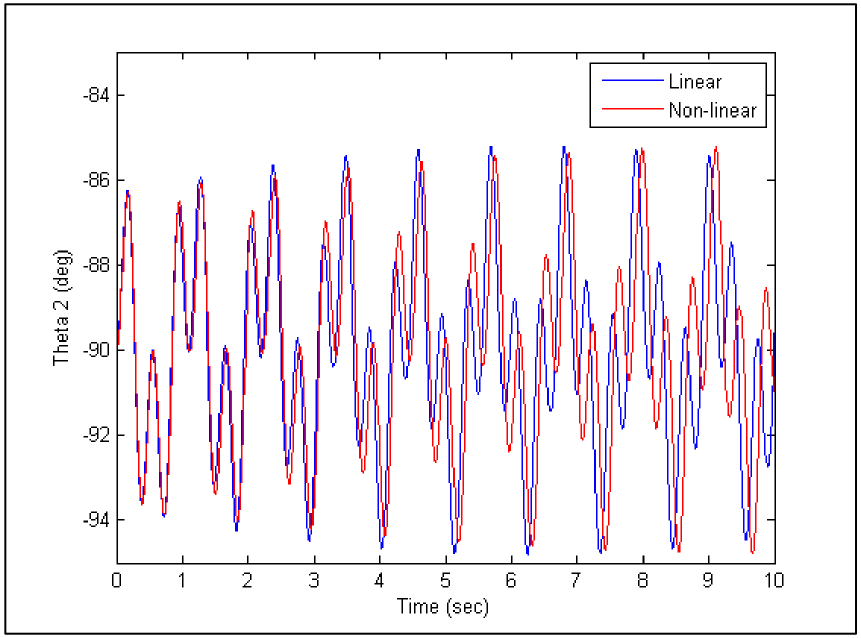

Response of joint 2 due to a non-equilibrium initial joint 3 angle of 10 degrees.

Dynamic Modeling: Linear Model

Comparison with Non-linear Model – Motor 3

Initial Joint 3 Angle of 5°

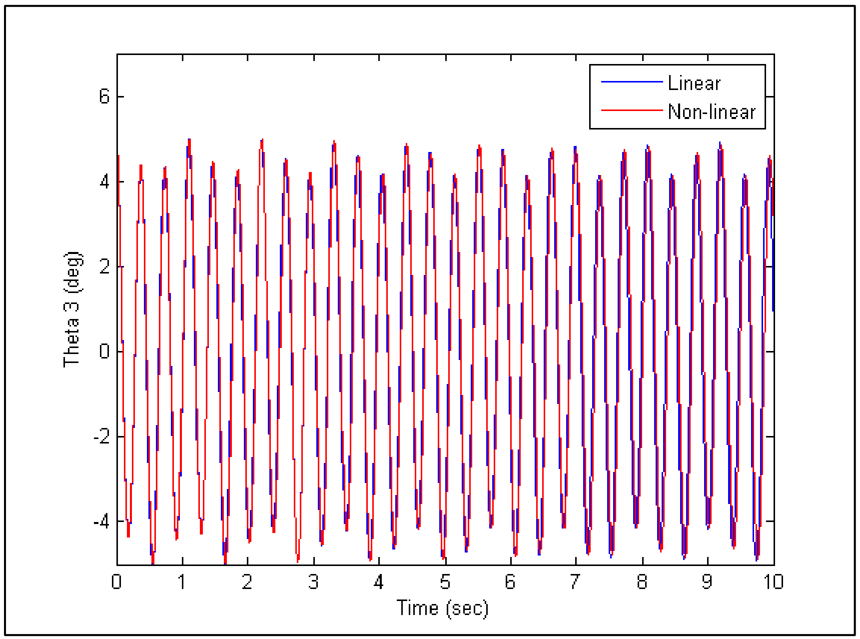

Response of joint 3 due to a non-equilibrium initial joint 3 angle of 5 degrees.

Initial Joint 3 Angle of 10°

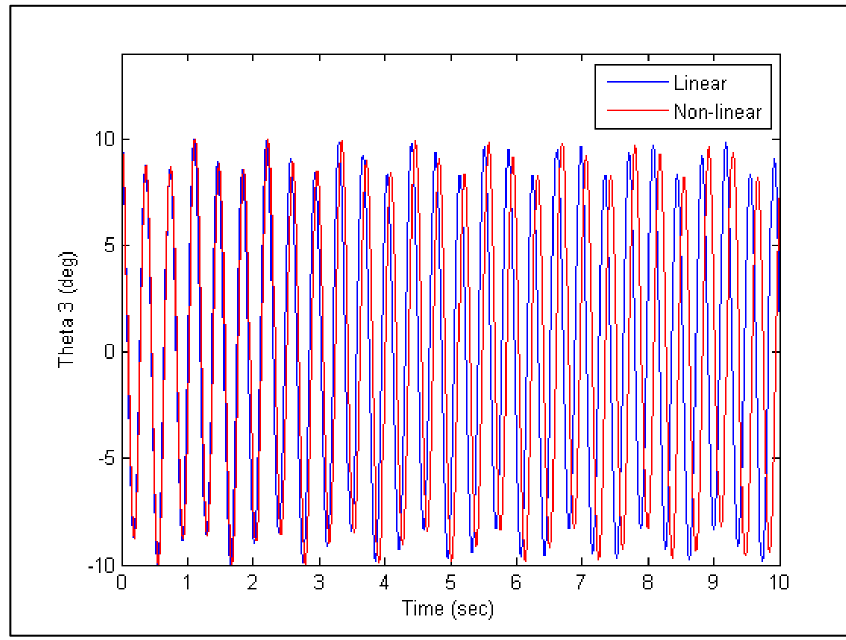

Response of joint 3 due to a non-equilibrium initial joint 3 angle of 10 degrees.

PID Controller

Block Diagram

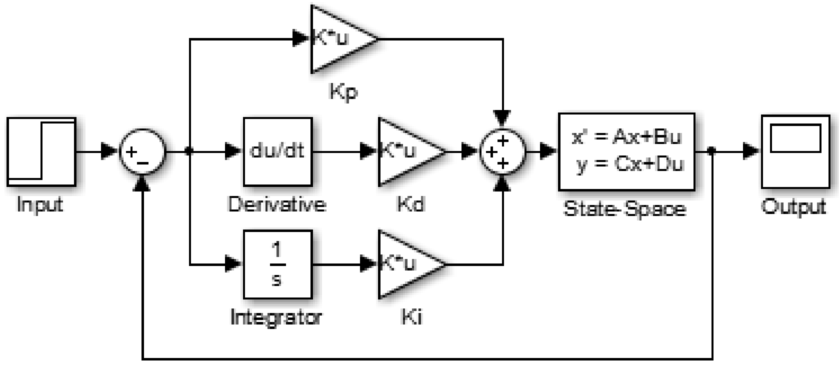

Block diagram of PID controller.

System Equation:

$$\tau = K_D \dot{E} + K_P E + K_i \int E dt$$

Error:

$$E = \theta_{desired} - \theta_{actual}$$

Motor 1 Results

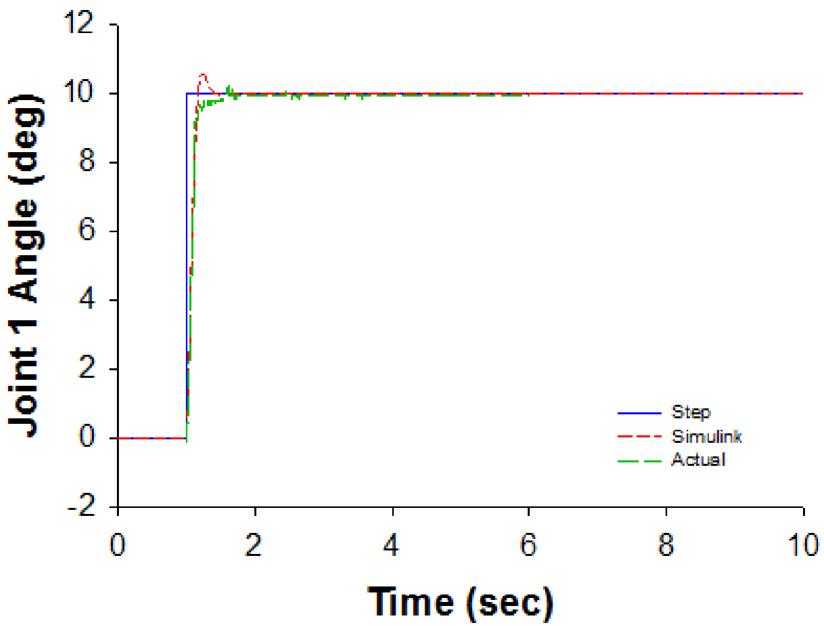

Comparison of theoretical response and actual response for motor 1.

PID Controller (cont.)

Motor 2 Results

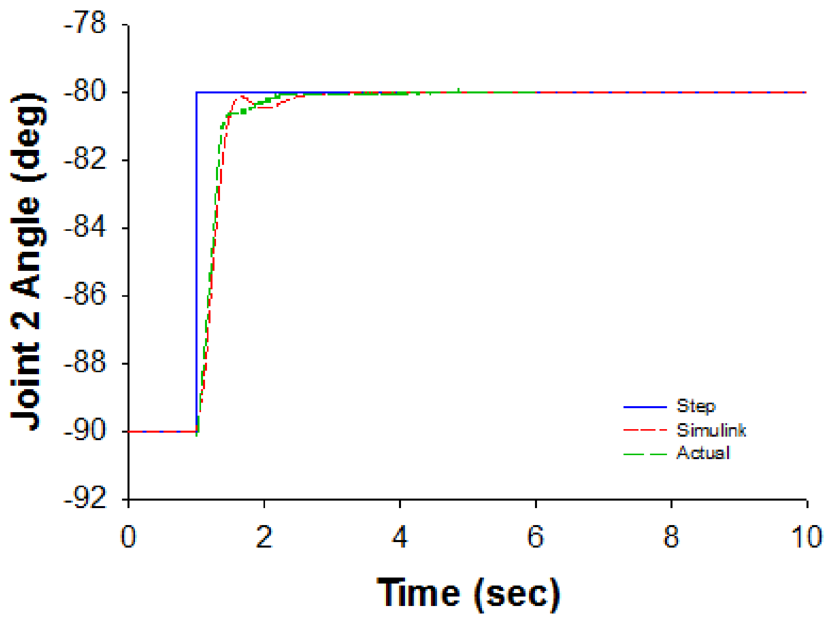

Comparison of theoretical response and actual response for motor 2.

Motor 3 Results

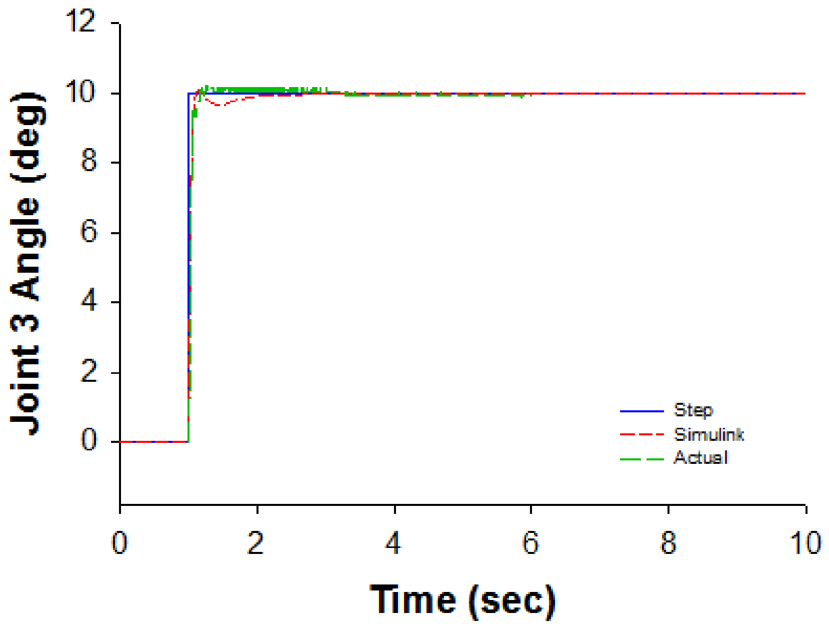

Comparison of theoretical response and actual response for motor 3.

Gravity Compensation

Forces Due to Weight of Robot and Human Arm

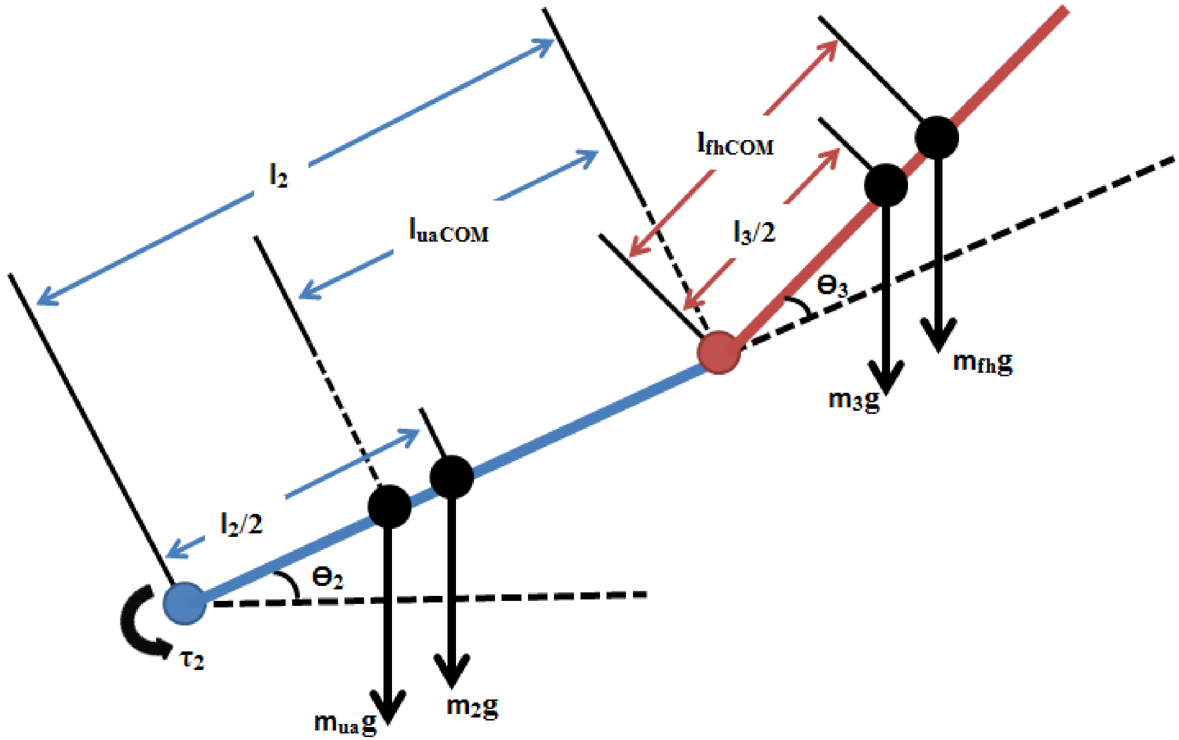

Free body diagram about joint 2 for static position.

$$\tau_2 = m_{ua}g\,(l_2 - l_{uaCOM})\cos\theta_2 + m_2 g\frac{l_2}{2}\cos\theta_2 + m_3 g\left(l_2\cos\theta_2 + \frac{l_3}{2}\cos(\theta_2+\theta_3)\right) + m_{fh}g\Big(l_2\cos\theta_2 + l_{fhCOM}\cos(\theta_2+\theta_3)\Big) \quad (21)$$

Gravity Compensation

Properties of Human Arm

Properties of Upper Arm[11]

Property	Value
Mass	1.73 kg
Center of Mass from Acromion (Shoulder)	17.13 cm
Location of Center of Mass as a Ratio of Segment Size	51.30

Properties of Forearm and Hand[11]

Property	Value
Mass	1.483 kg
Center of Mass from Radiale (Elbow)	16.21 cm
Location of Center of Mass as a Ratio of Segment Size	62.58

11. Clauser, Charles, John McConville, and J.W. Young. Weight, Volume, and Center of Mass of Segments of the Human Body. Wright-Patterson Air Force Base, Ohio: Aerospace Medical Research Laboratory, 1969.

Gravity Compensation

No Compensation with No Human Arm

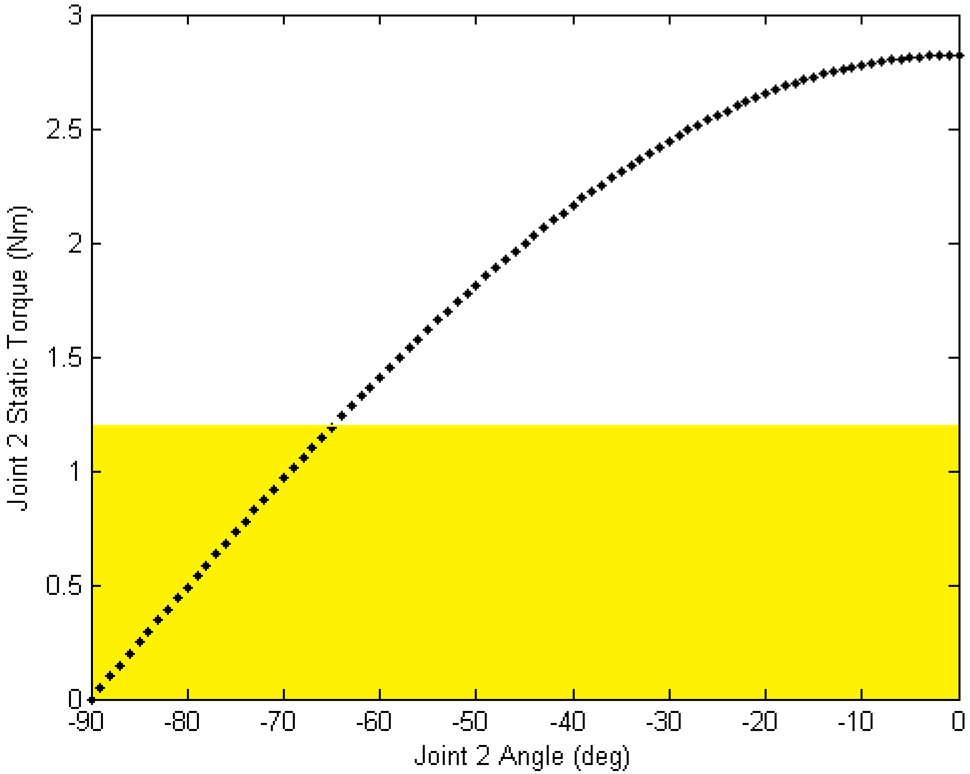

Static joint 2 torque for no limb.

Gravity Compensation
Add Constant Force Spring

Constant Force Spring

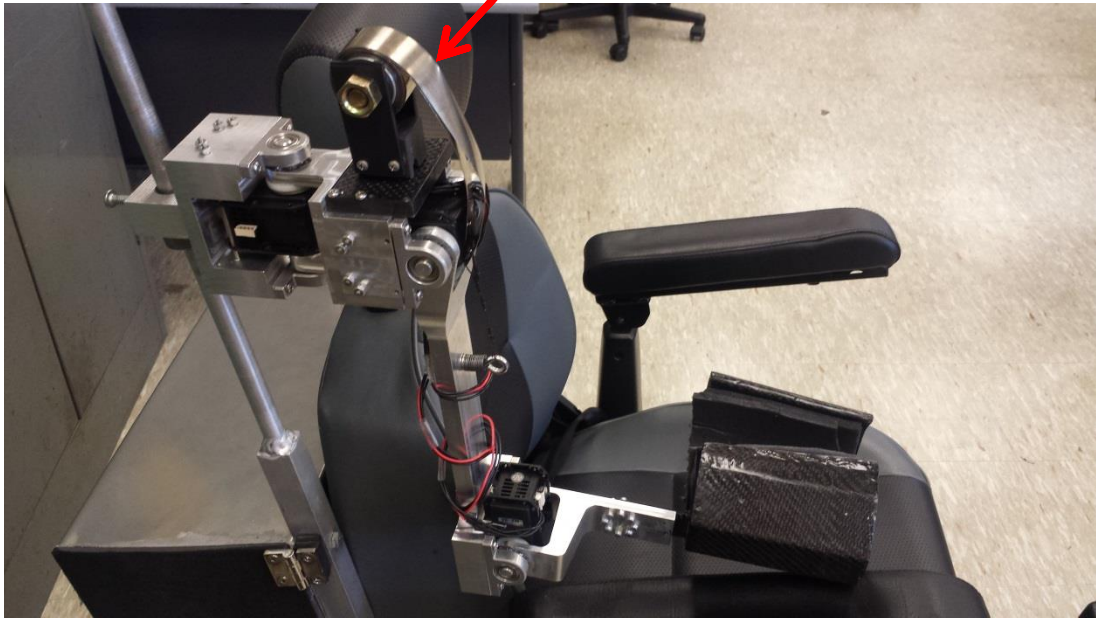

Side view of robotic arm with constant force spring.

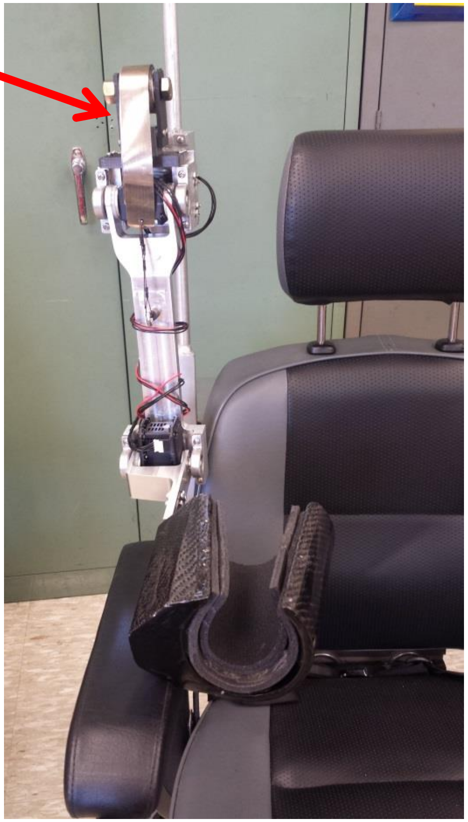

Front view of robotic arm with constant force spring.

Gravity Compensation

Added Force Due to Constant Force Spring

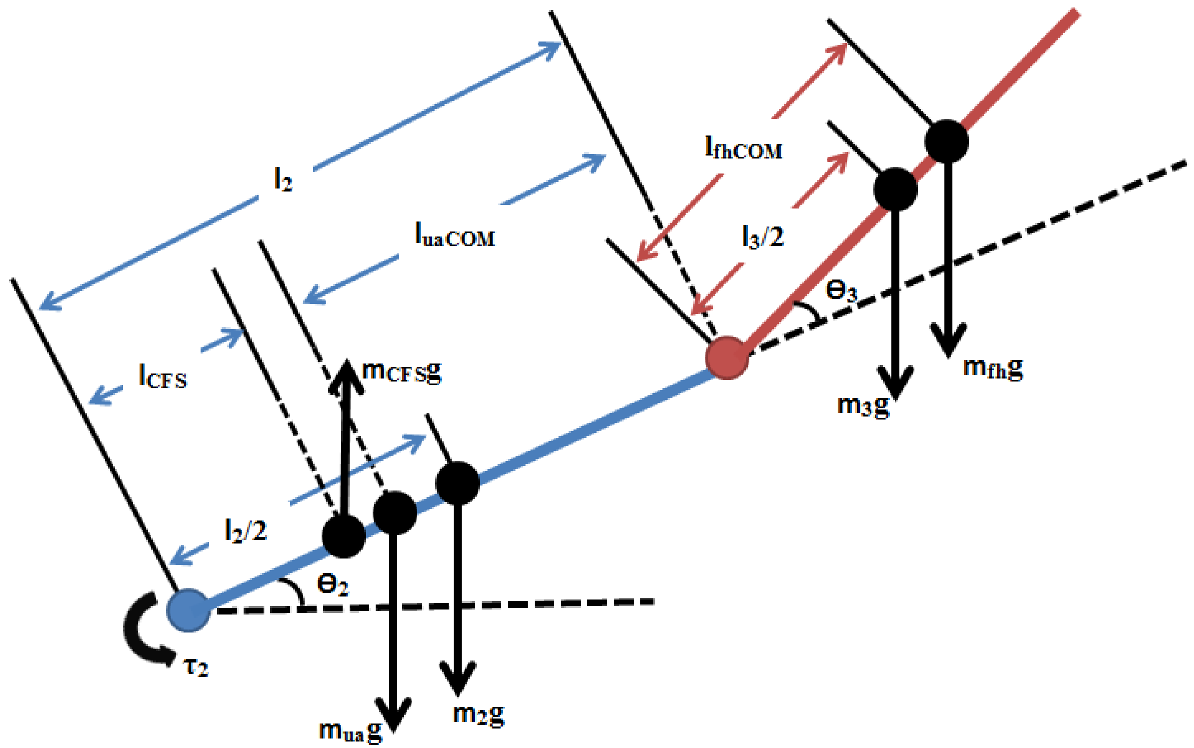

Free body diagram about joint 2 for static position with CFS.

$$\tau_2 = -m_{CFS} g l_{CFS} \cos\theta_2 + m_{ua} g \left(l_2 - l_{uaCOM}\right)\cos\theta_2 + m_2 g \frac{l_2}{2}\cos\theta_2 + m_3 g \left(l_2\cos\theta_2 + \frac{l_3}{2}\cos(\theta_2+\theta_3)\right) + m_{fh} g \Big(l_2\cos\theta_2 + l_{fhCOM}\cos(\theta_2+\theta_3)\Big) \quad (22)$$

Gravity Compensation

Added Force Due to Constant Force Spring (No Limb)

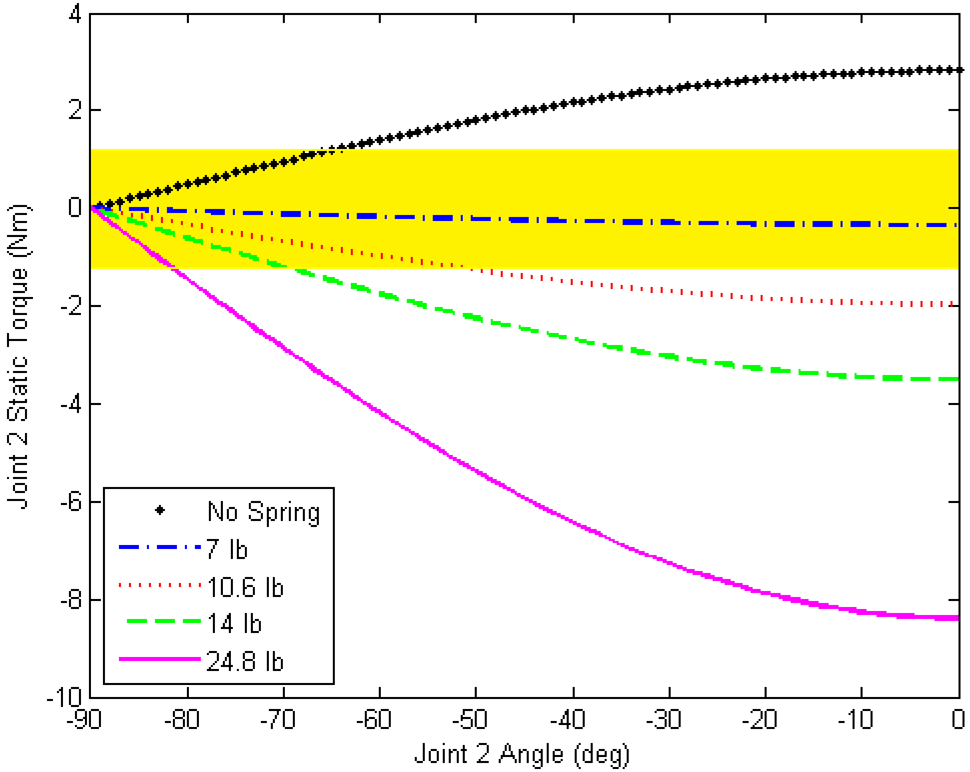

Static joint 2 torque with CFS for no limb.

Gravity Compensation

Added Forces Due to Constant Force Spring (With Limb)

Joint 3 Angle Fixed at Zero

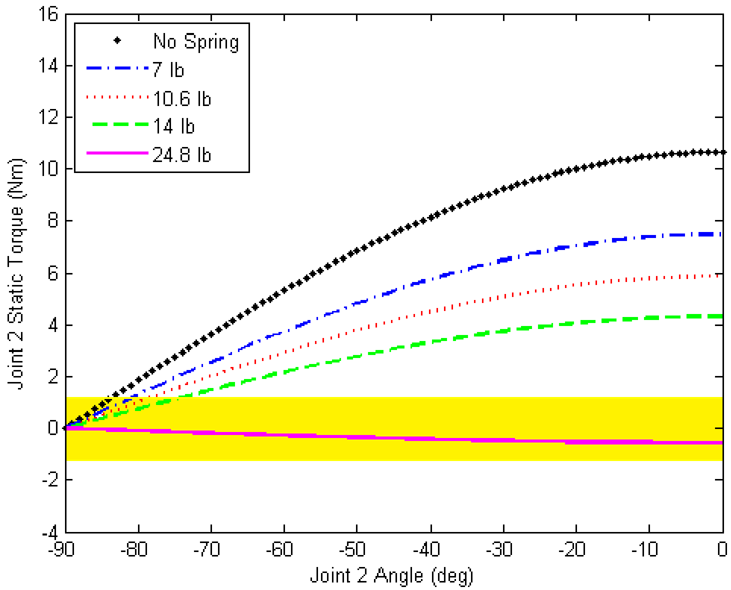

Static joint 2 torque with CFS and limb for joint 3 angle of zero.

Joint 2 Angle Fixed at Zero

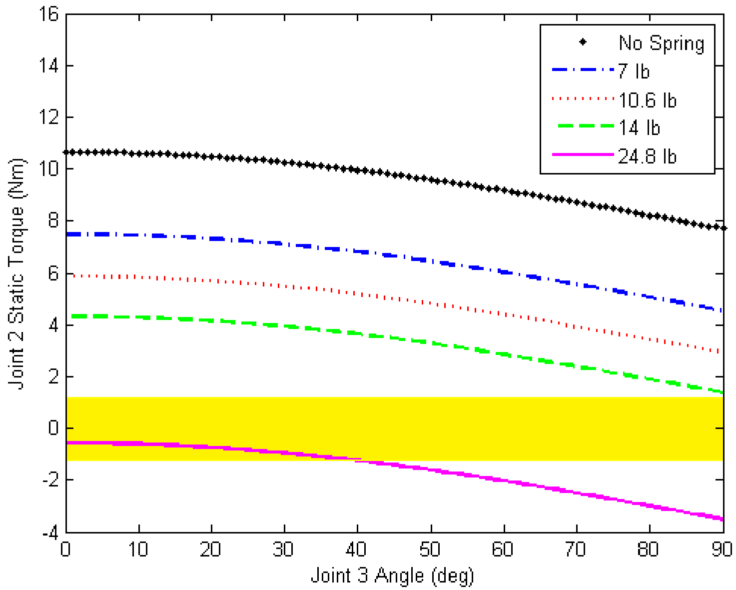

Static joint 2 torque with CFS and limb for joint 2 angle of zero.

User Intention: Torque Feedback

Reduce System to 2DOF

- Reasoning
  - Remove 3rd degree of freedom to simplify torque calculation about joint 2 (τ_2)
- Plan
  - Solve for τ_2 from Lagrangian
  - Compare theoretical joint torque results with actual joint torque results

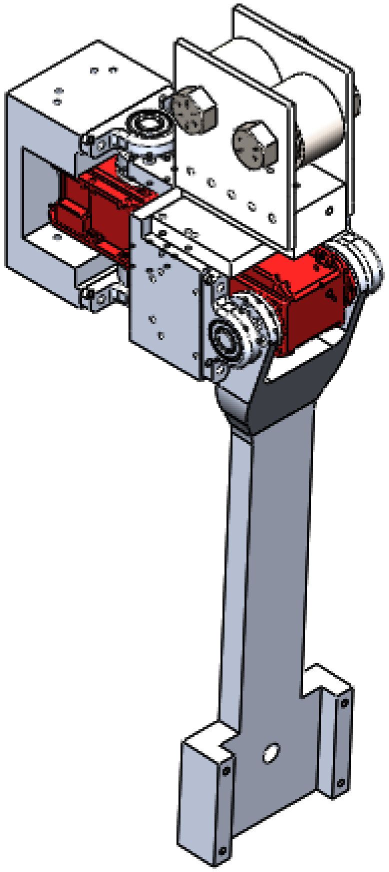

CAD model of 2DOF system.

User Intention: Torque Feedback

Sensor Calibration

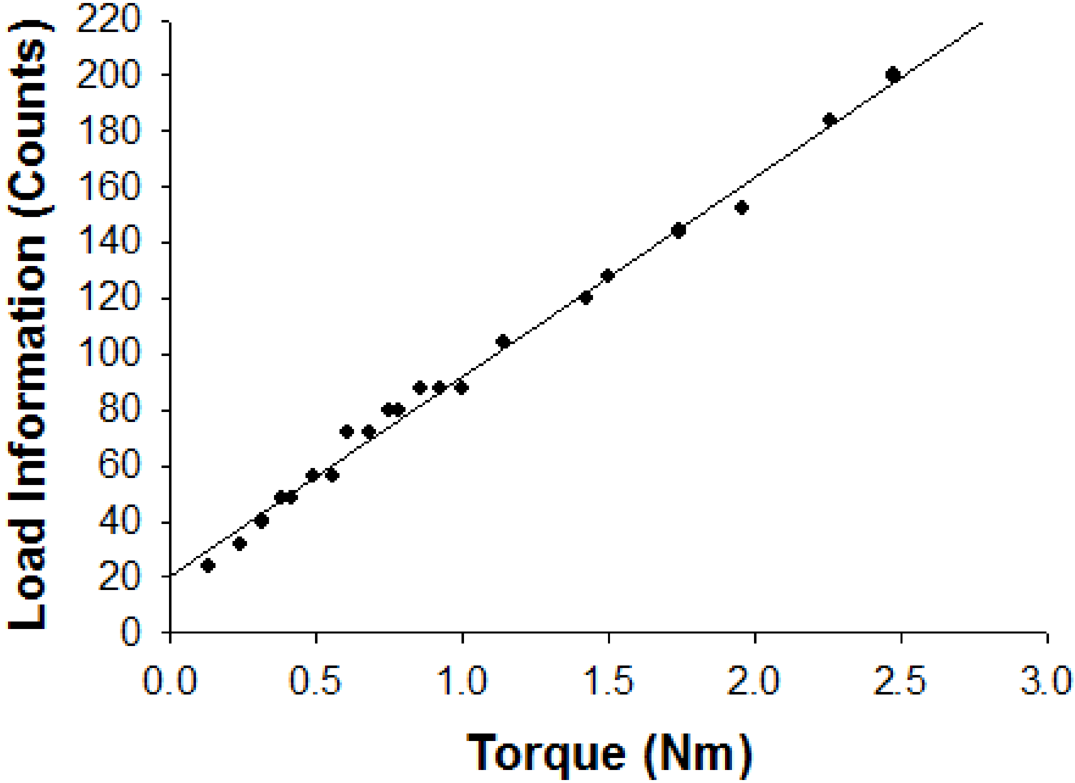

Torque sensor calibration.

User Intention: Torque Feedback

2DOF Joint Torques

Lagrangian: $$L(q,\dot{q}) = T(q,\dot{q}) - U(q) \tag{23}$$

Lagrangian with no Kinetic Energy: $$L = -U \tag{24}$$

Potential Energy for 2DOF System: $$U = -m_1 \vec{g}^{T\,0}\vec{r}_{c_1} - m_2 \vec{g}^{T\,0}\vec{r}_{c_2} \tag{25}$$

Potential Energy for 2DOF Expanded:

$$\begin{aligned}
U =& -m_1 \begin{bmatrix} 0 & 0 & -g \end{bmatrix} \begin{Bmatrix} L_{1_{COM_x}} \cos\theta_1 - L_{1_{COM_y}} \sin\theta_1 \\ L_{1_{COM_x}} \sin\theta_1 + L_{1_{COM_y}} \cos\theta_1 \\ L_{1_{COM_z}} \end{Bmatrix} \\
& - m_2 \begin{bmatrix} 0 & 0 & -g \end{bmatrix} \begin{Bmatrix} L_{2_{COM_x}} c\theta_1 c\theta_2 - L_{2_{COM_y}} c\theta_1 s\theta_2 + L_{2_{COM_z}} s\theta_1 + a_1 c\theta_1 \\ L_{2_{COM_x}} s\theta_1 c\theta_2 - L_{2_{COM_y}} s\theta_1 s\theta_2 - L_{2_{COM_z}} c\theta_1 + a_1 s\theta_1 \\ L_{2_{COM_x}} s\theta_2 + L_{2_{COM_z}} c\theta_2 \end{Bmatrix} \\
=& -m_1 \left[(-g) L_{1_{COM_z}}\right] - m_2 \left[(-g)(L_{2_{COM_x}} s\theta_2 + L_{2_{COM_y}} c\theta_2)\right] \\
=& m_1 g L_{1_{COM_z}} + m_2 g \left(L_{2_{COM_x}} s\theta_2 + L_{2_{COM_y}} c\theta_2\right)
\end{aligned} \tag{26}$$

User Intention: Torque Feedback

2DOF Joint Torques (cont.)

Euler-Lagrange:

$$\frac{d}{dt}\left[\frac{\partial L(q,\dot{q})}{\partial \dot{q}_i}\right] - \frac{\partial L(q,\dot{q})}{\partial q_i} = \tau_i, \qquad i = 1, \cdots, n \tag{27}$$

Joint Torque i:

$$\begin{aligned} \tau_i &= -\frac{\partial L}{\partial \theta_i} \\ &= \frac{\partial}{\partial \theta_i}\left[m_1 g L_{1_{COM_z}} + m_2 g \left(L_{2_{COM_x}} s\theta_2 + L_{2_{COM_y}} c\theta_2\right)\right] \end{aligned} \tag{28}$$

Joint Torque 1:

$$\begin{aligned} \tau_1 &= \frac{\partial}{\partial \theta_1}\left[m_1 g L_{1_{COM_z}} + m_2 g \left(L_{2_{COM_x}} s\theta_2 + L_{2_{COM_y}} c\theta_2\right)\right] \\ &= 0 \end{aligned} \tag{29}$$

Joint Torque 2:

$$\begin{aligned} \tau_2 &= \frac{\partial}{\partial \theta_2}\left[m_1 g L_{1_{COM_z}} + m_2 g \left(L_{2_{COM_x}} s\theta_2 + L_{2_{COM_y}} c\theta_2\right)\right] \\ &= m_2 g \left(L_{2_{COM_x}} c\theta_2 - L_{2_{COM_y}} s\theta_2\right) \end{aligned} \tag{30}$$

User Intention: Torque Feedback

Results

Motor 1

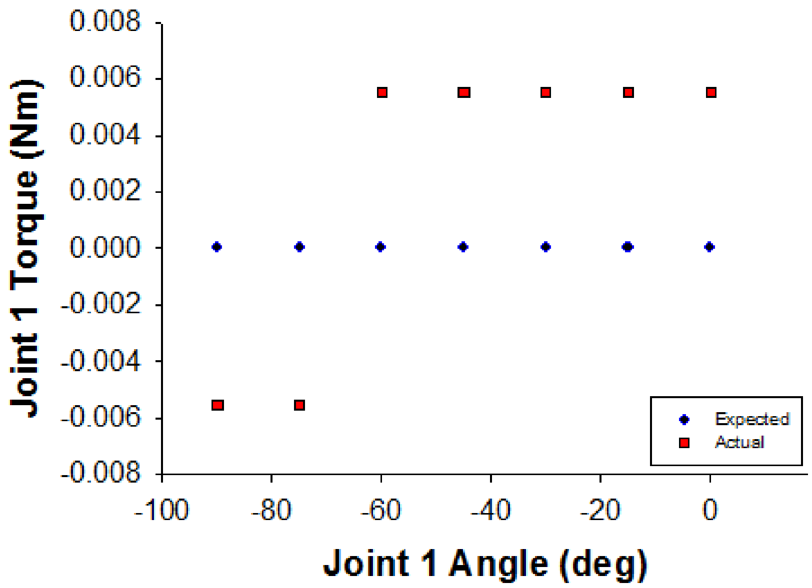

Comparison of theoretical joint torque and actual joint torque for motor 1.

Motor 2

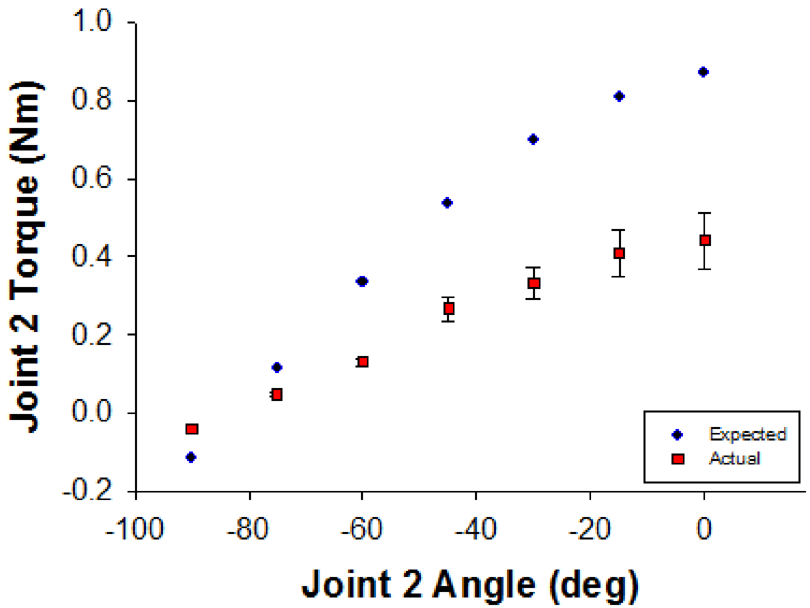

Comparison of theoretical joint torque and actual joint torque for motor 2.

User Intention: Torque Feedback

Load Information vs Position Information

Motor 1

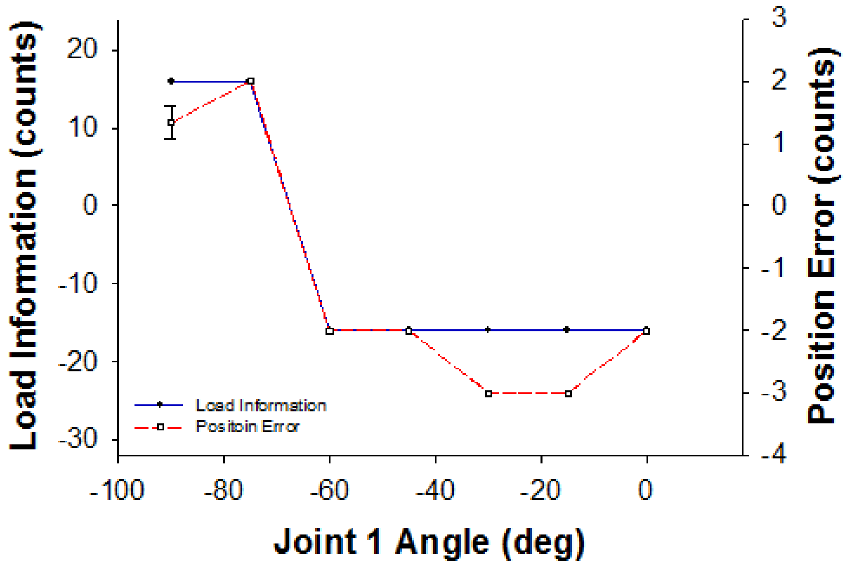

Load information compared to position error for motor 1.

Motor 2

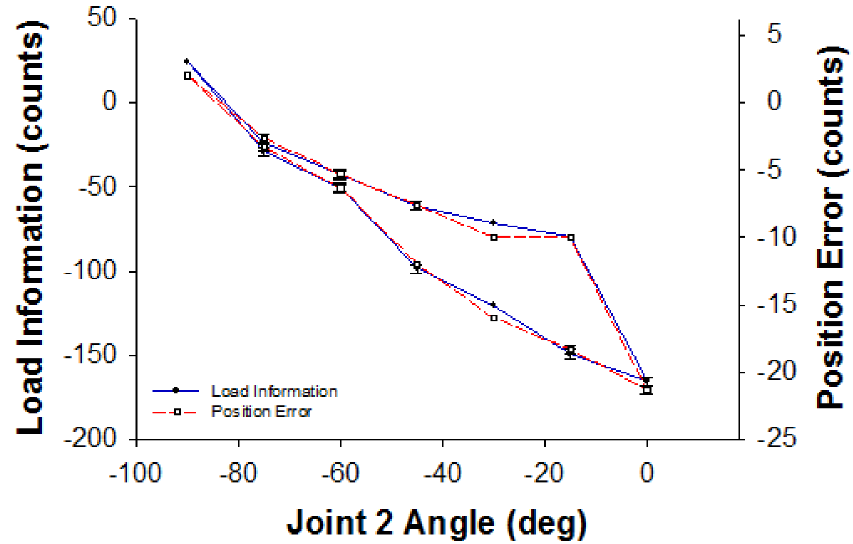

Load information compared to position error for motor 2.

User Intention: EMG Feedback

Sensor Placement for Wrist Extension

Extensor Carpi Ulnaris

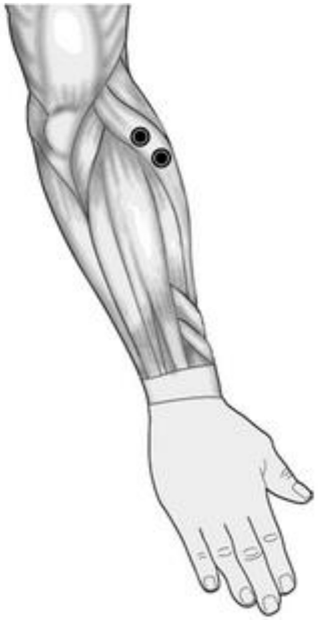

EMG sensor placement for extensor carpi ulnaris muscle[12].

Wrist Extension

Example of wrist extension[13].

12. Cram, Jeffrey, Glenn Kasman, and Jonathan Holtz. "Atlas for Electrode Place- ment." In Cram's Introduction to Surface Electromyography, edited by Eleanor Criswell, 245-383. Sudbury: Jones and Bartlett Publishers, 2011.
13. University of Michigan. "Movements of the Upper Limb." Learning Modules - Medical Gross Anatomy. Ann Arbor, 2002.

User Intention: EMG Feedback

Sensor Placement for Wrist Flexion

Flexor Carpi Ulnaris

EMG sensor placement for flexor carpi ulnaris muscle[14].

Wrist Flexion

Example of wrist flexion[15].

14. Cram, Jeffrey, Glenn Kasman, and Jonathan Holtz. "Atlas for Electrode Place- ment." In Cram's Introduction to Surface Electromyography, edited by Eleanor Criswell, 245-383. Sudbury: Jones and Bartlett Publishers, 2011.
15. University of Michigan. "Movements of the Upper Limb." Learning Modules - Medical Gross Anatomy. Ann Arbor, 2002.

User Intention: EMG Feedback

Results for Wrist Extension

Raw EMG

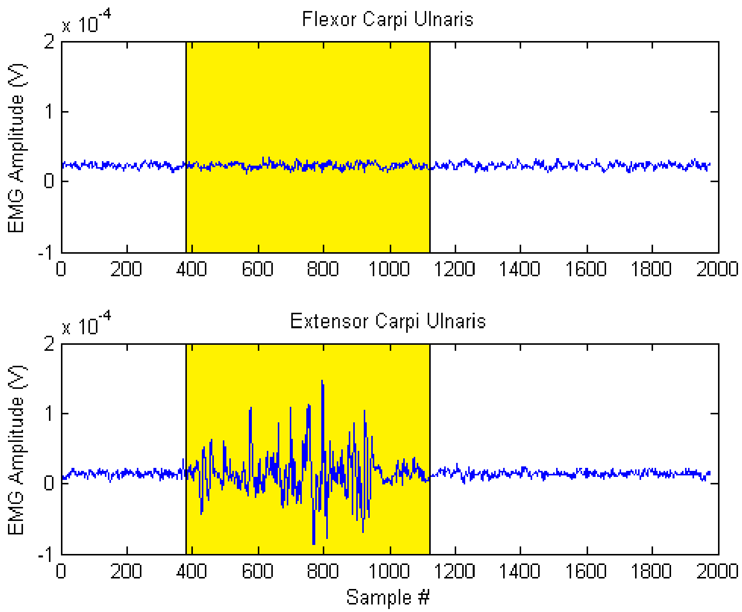

Raw EMG of flexor carpi ulnaris and extensor carpi ulnaris muscles during wrist extension.

EMG Squared

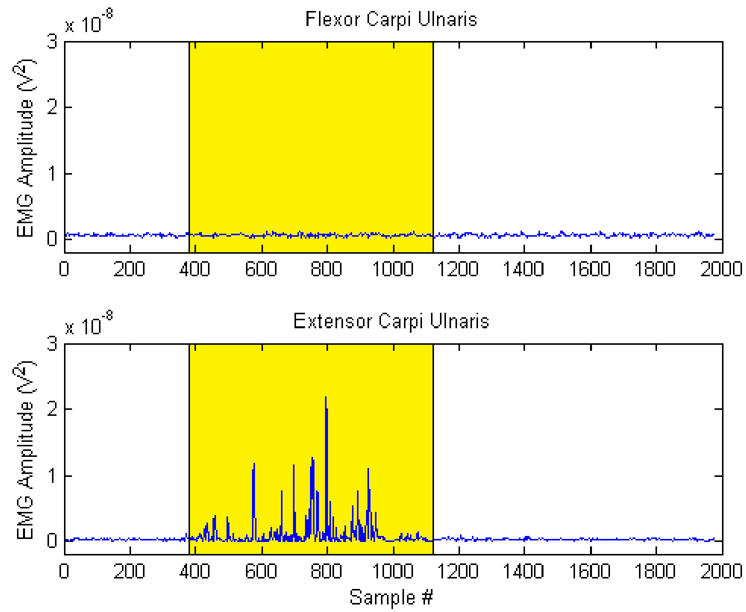

Squared EMG of flexor carpi ulnaris and extensor carpi ulnaris muscles during wrist extension.

User Intention: EMG Feedback

Results for Wrist Flexion

Raw EMG

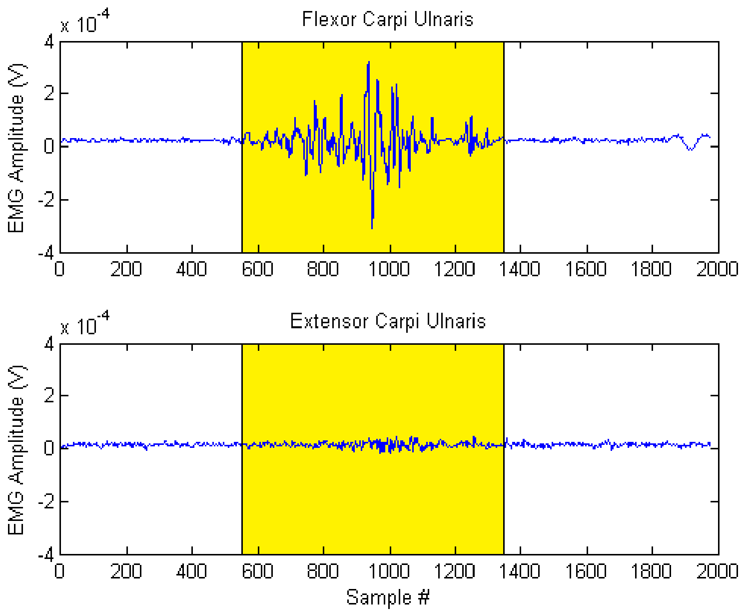

Raw EMG of flexor carpi ulnaris and extensor carpi ulnaris muscles during wrist flexion.

EMG Squared

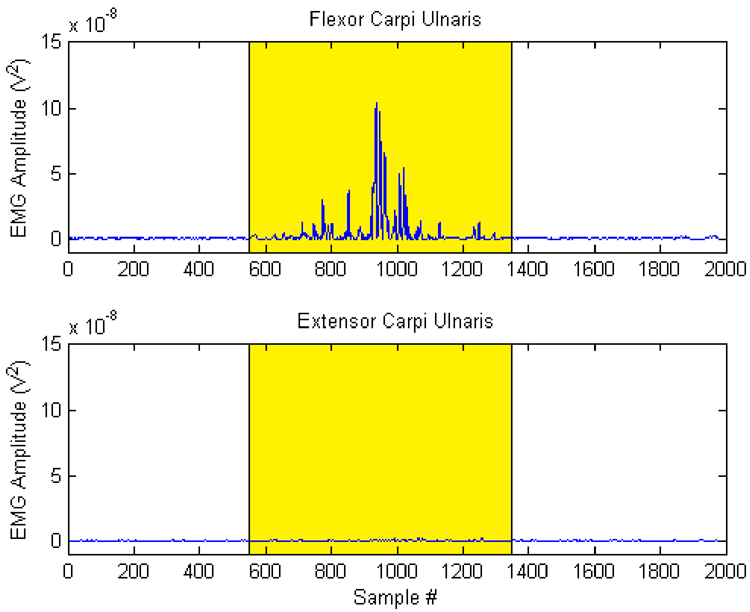

Squared EMG of flexor carpi ulnaris and extensor carpi ulnaris muscles during wrist flexion.

Conclusion

- Importance
  - Growing need of wearable robots in healthcare
- Research
  - Lightweight device at the expense of torque
    - Tradeoff between portability and power
    - Constant force spring not enough to compensate
  - User Intent
    - Torque sensors do not provide a large enough resolution and are not accurate enough
    - Biosignals are a much more reliable method of determining user intent

Future Work

- Improve model by including friction
  - Difficult to measure
  - Friction has many factors
  - Non-linear phenomenon
- Improve control by including actuator dynamics:
  - Including actuator dynamics makes system 3rd order
  - Tradeoff between model accuracy and controller simplicity
- Torque compensation for joint 2
  - Different motor
    - Possible option: Dynamixel Pro Series

QUESTIONS?